

A PROBABILISTIC FATIGUE ANALYSIS OF MULTIPLE SITE DAMAGE

S.M. Rohrbaugh¹, D. Ruff², B.M. Hillberry³, G. McCabe⁴
and A.F. Grandt, Jr.⁵
Purdue University
West Lafayette, IN 47907 USA

113060

ABSTRACT

The variability in initial crack size and fatigue crack growth is incorporated in a probabilistic model that is used to predict the fatigue lives for unstiffened aluminum alloy panels containing multiple site damage (MSD). The uncertainty of the damage in the MSD panel is represented by a distribution of fatigue crack lengths that are analytically derived from equivalent initial flaw sizes. The variability in fatigue crack growth rate is characterized by stochastic descriptions of crack growth parameters for a modified Paris crack growth law. A Monte-Carlo simulation explicitly describes the MSD panel by randomly selecting values from the stochastic variables and then grows the MSD cracks with a deterministic fatigue model until the panel fails. Different simulations investigate the influences of the fatigue variability on the distributions of remaining fatigue lives. Six cases that consider fixed and variable conditions of initial crack size and fatigue crack growth rate are examined. The crack size distribution exhibited a dominant effect on the remaining fatigue life distribution, and the variable crack growth rate exhibited a lesser effect on the distribution. In addition, the probabilistic model predicted that only a small percentage of the life remains after a lead crack develops in the MSD panel.

INTRODUCTION

Multiple site damage (MSD) refers to the accumulation of widespread fatigue cracking in aircraft structural details. MSD can be especially damaging when cracks initiate at several adjacent fastener holes in a mechanically fastened joint. Over time, the effects of the fatigue damage will reduce the residual strength of an aircraft joint and may result in a loss of damage tolerance capability. To reliably predict the capability of an MSD joint, the influences of widespread fatigue cracking and the associated crack growth mechanisms are needed.

The development of a method that incorporates the randomness in widespread fatigue cracking lends itself to a probabilistic approach. The initial crack sizes in the MSD joint can be

¹ Graduate Research Assistant, School of Mechanical Engineering
² Graduate Research Assistant, Department of Statistics
³ Professor, School of Mechanical Engineering
⁴ Professor, Department of Statistics
⁵ Professor, School of Aeronautics and Astronautics

represented by randomly selecting crack lengths from an analytically or experimentally derived distribution. The distribution of fatigue crack sizes can be estimated using an equivalent initial flaw size (EIFS) method proposed by Manning and Yang [1-5]. In addition to different MSD crack lengths, each crack is expected to grow at a different rate as observed by Virkler et al. [6]. Ostergaard and Hillberry [7] derived the distributions for the fatigue crack growth parameters that described the variability observed by Virkler. From the development of accurate descriptions of the crack sizes and crack growth rate as described above, a probabilistic model can be implemented to determine the influence of these random variables on fatigue life predictions. This approach can then be applied to an unstiffened panel containing MSD cracks to provide a better understanding of the effects of widespread fatigue cracking. A model of an unstiffened MSD panel was developed by Moukawsher et al. [8-11]. Moukawsher's model deterministically calculates fatigue crack growth, incorporates crack interaction effects, and predicts panel failure. This MSD fatigue model is integrated into a probabilistic model to determine a distribution of fatigue lives for a panel containing MSD cracks.

The objectives of this study are: (1) to characterize the variables associated with widespread fatigue cracking, (2) to develop a probabilistic method that incorporates the randomness for these variables, and (3) to evaluate the influence of fatigue variability on life predictions for an aluminum alloy panel containing MSD cracks. The present goal is to observe trends in fatigue lives of panels that contain both multiple site damage on the scale observed in aging aircraft and realistic crack growth properties of the material that was used to build these aircraft.

MATERIALS AND METHODS

Multiple Site Damage Model

The multiple site damage model considered here is a panel 787 mm wide by 2.3 mm thick containing 30 holes 4.76 mm in diameter (Figure 1). The holes are equally spaced and aligned perpendicular to the applied loading. This geometry was also considered by Buhler et al. [11] in a parametric study which employed the deterministic MSD analysis developed by Moukawsher et al. [8-10]. For this study the panel material considered was 2024-T3 aluminum alloy. The initial damage state was through-the-thickness cracks emanating from each side of the 30 holes. The panel was subjected to a constant amplitude remote tension of 68.9 MPa and a stress ratio of 0.1. Failure of the panel was considered to be fracture. A residual strength criterion based on Swift's ligament yield model [12] was used to predict failure. Moukawsher et al. [9,10] experimentally tested 2024-T3 aluminum alloy panels with MSD and observed good agreement with the residual strength criterion.

Variability in Initial Crack Size

The initial fatigue cracks at the holes in the panel were represented by an analytically derived distribution of crack sizes. The Manning and Yang approach for predicting fatigue cracking in aircraft from equivalent initial flaw size distributions was followed [1-5]. An EIFS distribution represents a population of artificial cracks, which when grown forward will be similar to

observed fatigue cracking in aircraft. An EIFS is a derived quantity and not necessarily equivalent to the actual flaw sizes at the time of manufacture. EIFS values are determined by back extrapolating fractographic data to a service time $t=0$ by integrating the analytical crack growth rate model given by equation 1,

$$\frac{da(t)}{dt} = Q \cdot a(t) \quad (1)$$

where $da(t)/dt$ is the crack growth rate, a is the crack size in millimeters, Q is the crack growth rate coefficient per hour, and t is the service time. The EIFS values are then fit to a Weibull compatible distribution function

$$F(a) = \exp \left\{ - \left[\frac{\ln(x_u/a)}{\phi} \right]^\alpha \right\} \quad (2)$$

where x_u is an upper-bound, α is the scale parameter, and ϕ is the shape parameter.

Widespread fatigue cracking in aircraft is predicted by growing the EIFS distribution (equation 2) forward to some service time $t=T$. To simplify the analysis, the service crack growth curve (SCGC) for a given stress region of an aircraft is estimated with the analytical crack growth rate equation (equation 1). A reasonable approximation is achieved by fitting the analytical equation in two-segments to the SCGC according to a reference crack size (a_0) as shown below:

$$\frac{da}{dt} = Q_1 \cdot a^{b_1} \quad a(t) < a_0 \quad (3)$$

$$\frac{da}{dt} = Q_2 \cdot a^{b_2} \quad a(t) \geq a_0 \quad (4)$$

The crack growth coefficients Q_1 and Q_2 for a given SCGC are estimated from equations 5 and 6,

$$Q_1 = \xi_1 \cdot \sigma^{\psi_1} \quad (5)$$

$$Q_2 = \xi_2 \cdot \sigma^{\psi_2} \quad (6)$$

where σ is the maximum stress level of the SCGC in MPa, and $\xi_1, \xi_2, \psi_1, \psi_2$ are empirical constants based on crack size data observed fractographically. The crack growth exponents b_1 and b_2 were equal to one in this study as suggested by Manning and Yang [1,2]. Once the crack growth coefficients have been estimated for a given SCGC, the EIFS distribution can be analytically grown forward to determine the distribution of crack sizes at some service time $t=T$.

The EIFS approach was used by Yang and Manning in the durability analysis of a fighter lower wing skin [1]. The EIFS distribution parameters and empirical constants were determined from fractographic data sets for laboratory specimens under spectrum loading. The resulting EIFS distribution parameters for equation 2 were $x_u=0.762$ mm, $\alpha=1.716$, $\phi=6.308$, and the constants for equations 5 and 6 were $\xi_1=2.227E-19$, $\xi_2=6.288E-8$, $\psi_1=6.374$, and $\psi_2=1.546$. The crack growth coefficients (Q_1 and Q_2) were then estimated for ten different stress regions in the wing skin from equations 5 and 6. The analytically derived EIFS distribution can then be grown

forward by integrating equations 3 and 4 for each wing skin region to determine a distribution of crack sizes at any service time $t=T$.

Data reported by Yang and Manning [1] for the fighter lower wing skin were used in this study to generate the prediction for the extent of widespread fatigue cracking. The EIFS distribution was grown forward to 10,000 flight hours for stress region VI. The resulting fatigue crack sizes were then fit to a Weibull compatible distribution function (equation 2) with parameters $x_u=4.27$ mm, $\alpha=1.995$, and $\phi=6.921$. This analytically derived distribution is used to represent the initial crack sizes in the MSD panel.

Variability in Fatigue Crack Propagation

The variability in fatigue crack growth behavior was observed by Virkler et al. [6] for 68 replicate, constant amplitude tests of 2024-T3 aluminum alloy panels (Figure 2). Virkler measured the fatigue crack growth (a vs. N) in center cracked panels cut from the same material lot. The data were readily described by a modified Paris law [7]

$$\frac{da}{dN} = C \cdot (\Delta K - \Delta K_{th})^m \quad (7)$$

where the crack growth rate parameters C and m are material constants, da/dN is the crack growth rate in inches/cycle, ΔK is the stress intensity range in $\text{ksi}\sqrt{\text{in}}$, and ΔK_{th} is the threshold stress intensity. The threshold stress intensity value used by Ostergaard and Hillberry [7] and in this study was $2.75 \text{ ksi}\sqrt{\text{in}}$. Ostergaard and Hillberry [7] used a finite integral optimization (FIO) method to determine the fatigue crack growth rate parameters such that upon integration of equation 7 the original a vs. N data were accurately reproduced. The FIO method optimizes each parameter set by determining the C_i and m_i that give the best-fit to the a vs. N data according to a prescribed minimum error function.

From the 68 sets of optimized values for the crack growth parameters C_i and m_i , Ostergaard used a least-squares regression analysis of the $\log m$ vs. $\log C$ data to show that the mean crack growth behavior could be described by equation 8,

$$\log \hat{C}_i = b_0 + b_1 \cdot \log m_i \quad (8)$$

with mean crack growth parameter \hat{C}_i . The least-squares estimates were $b_0 = -5.7792$ and $b_1 = -4.6150$. The deviations of the fitted value $\log \hat{C}_i$ (from equation 8) compared to $\log C$ were used to describe the variability in crack growth rate. This variability was characterized by the parameter F defined below

$$F_i = \frac{\hat{C}_i}{C_i} \quad (9)$$

$$\log F_i = -(\log C_i - \log \hat{C}_i) \quad (10)$$

where the logarithm of F_i represents the least-squares residuals from the regression analysis. The results are two independent crack growth parameters m_i and F_i that describe the variability in the fatigue crack growth rate.

The derived m_i and F_i values from the a vs. N data showed a best-fit of the F parameter to the 3-parameter log-normal distribution function,

$$f(F) = \frac{1}{(F-\tau)\sqrt{2\pi\beta}} \cdot \exp\left(-\frac{1}{2\beta} \{\log(F-\tau) - \alpha\}^2\right) \quad (11)$$

where the scale, shape and threshold parameters were estimated to be $\alpha = -0.737$, $\beta = 0.025$, and $\tau = 0.807$ respectively. The m parameter showed a best-fit to the 2-parameter log-normal distribution function,

$$f(m) = \frac{1}{m\sqrt{2\pi\beta}} \cdot \exp\left(-\frac{1}{2\beta} \{\log m - \alpha\}^2\right) \quad (12)$$

where the scale and shape parameters are $\alpha = 0.35508$, and $\beta = 7.1162E-4$ respectively. The stochastic descriptions in equations 8-12 are used in the probabilistic model to represent the variability in fatigue crack growth rate.

Probabilistic Modeling

An important aspect in probabilistic modeling is to use a mechanistic approach that describes the fatigue process. The MSD fatigue model developed by Moukawsher et al. [8-11] provides a fracture mechanics approach to predict the fatigue life of a remotely loaded panel containing MSD cracks. The model incorporates the location, length, type of crack, and crack interaction effects in the calculation of the stress intensity factor (ΔK) solution for each crack. The corresponding crack growth rate is calculated from the da/dN vs. ΔK relationship, in this case a modified Paris law. The remaining fatigue life of the MSD panel is predicted by deterministically growing the cracks until the panel fails according to a residual strength criterion.

A Monte-Carlo simulation incorporates the fatigue variability with the MSD fatigue model described above to determine a distribution of remaining fatigue lives for the MSD panel. This probabilistic approach is used to investigate the influences of the variability in fatigue behavior and fatigue crack sizes by comparing different simulation conditions. The crack conditions considered were: 1) mean size cracks emanating from both sides of each fastener hole, 2) a random symmetric crack size emanating from both sides of each fastener hole, and 3) a random unsymmetric crack size emanating from both sides of each fastener hole. The crack growth rate conditions considered were: 1) mean crack growth parameters, 2) random crack growth parameters for each panel (homogeneous panel), and 3) random crack growth parameters at every ligament for each panel (heterogeneous panel).

Six Monte-Carlo simulations of 1000 trials each were investigated for the three crack size conditions and the three fatigue crack growth rate conditions. The influence of the fatigue variability was considered by evaluating simulations with different conditions of one fatigue

variability, while holding the other variability the same. The different simulation cases are described below, and are identified in Table 1.

- Case 1: mean crack sizes emanating from both sides of each hole and a randomly selected crack growth rate for each panel.
- Case 2: randomly selected symmetric crack sizes and a mean crack growth rate for each panel.
- Case 3: randomly selected unsymmetric crack sizes and a mean crack growth rate for each panel.
- Case 4: randomly selected symmetric crack sizes and a randomly selected crack growth rate for each panel.
- Case 5: randomly selected unsymmetric crack sizes and a randomly selected crack growth rate for each panel.
- Case 6: randomly selected symmetric crack sizes and a randomly selected crack growth rate at every ligament for each panel.

By direct comparison of the fatigue life distributions for these cases, the fatigue life variability can be quantified to provide a better understanding of the uncertainties in the MSD panel.

Table 1. Monte-Carlo Combinations of the MSD Panel

Case	Crack size parameter	Material parameter
1	mean crack size every hole	variable crack growth rate each panel
2	variable symmetric crack size every hole	mean crack growth rate each panel
3	variable unsymmetric crack size every hole	mean crack growth rate each panel
4	variable symmetric crack size every hole	variable crack growth rate each panel
5	variable unsymmetric crack size every hole	variable crack growth rate each panel
6	variable symmetric crack size every hole	variable crack growth rate every hole

RESULTS AND DISCUSSION

The six Monte-Carlo simulations predicted stochastically tight distributions for the remaining fatigue lives of the MSD panels (Figures 3-8). To directly compare the different cases, the means and standard deviations are plotted in a bar chart for each case (Figure 9). *Case 1 vs. 4* compares the mean crack sizes and the randomly selected crack sizes for the same crack growth rate condition. In this comparison, the mean fatigue life decreased significantly for the randomly selected cracks due to cracks larger than the mean value interacting with the adjoining cracked holes. As a result, a dominant crack would link-up to form a lead crack, whereby the panel would fail soon thereafter as a result of the loss in residual strength. *Case 2 vs. 4* compares the mean crack growth rate with the randomly selected crack growth rate for the same initial crack size condition. No significant difference in the mean fatigue lives occurred; however, the standard deviation increased with the addition of the variable crack growth. This suggests that the mean fatigue life is not sensitive to the variability in fatigue crack growth rate, but the shape of the distribution is affected. *Case 4 vs. 6* compares the variable crack growth rate for each panel and the variable crack growth rate for each ligament in the panel. Both cases exhibited similar distributions which support the previous observations. *Case 2 vs. 3* and *Case 4 vs. 5* compares the symmetric crack sizes and the unsymmetric crack sizes. These comparisons show an increase in the mean fatigue lives and a decrease in the standard deviation for the unsymmetric crack conditions. The increase in mean life is expected since a large crack that is symmetric is more damaging than a large/small unsymmetric crack condition. Overall, the crack size distribution exhibited a dominant effect on the fatigue life predictions, and the variable crack growth rate exhibited a lesser effect on the fatigue life predictions. Due to the panel containing a large number of consecutive holes, the probability increased that each panel would contain a large flaw. This combined influence of the number of holes and the fatigue variability on the life distribution warrants further investigation.

Panel failure occurred in *Cases 2-6* as a result of the formation of a lead crack reducing the residual strength of the panel. This behavior was investigated by calculating the percent remaining life after the first link-up. Histogram plots of the percentages are shown in Figures 10 through 14. Comparing the means and standard deviations for each case in the bar chart (Figure 15) shows that approximately 5% of the life remains after the development of a lead crack. This suggests that the majority of the life is spent propagating the initial cracks; therefore, a reliable analysis must include a good representation of the input variables. The uniform cracking in *Case 1* never developed a lead crack and the panel failed from net section yielding.

The utility in analyzing trends between different cases depends on appropriately representing the fatigue variabilities in the MSD panel. It was determined that for the analytically derived crack size distribution that approximately 33% of the cracks would propagate. This is a result of the modified Paris crack growth equation (equation 7) preventing cracks from growing at stress intensities below the threshold value. The derived crack size distribution in the MSD panel at 10,000 flight hours was compared to observed crack size data reported by Lincoln [13] for 19 trainer aircraft. Lincoln reported the destructive tear down and inspection of trainer wings revealing 25-50% of the fastener holes had detectable cracks. Additionally, the initial crack size distribution for this study compares favorably with the fitted distribution to the observed cracks found in the trainer aircraft (Figure 16). The distributions of fatigue crack growth parameters were developed from a 2024-T3 aluminum alloy produced in 1976 which is of the same vintage as the material used in the aging aircraft fleet.

Although the current paper has expressed the results of the probabilistic MSD analysis in terms of remaining fatigue life distributions, the approach could also be used to determine the variation in residual strength as a function of elapsed cycles. In that case, Monte-Carlo

simulations would be performed as before to predict distributions in MSD crack patterns at various predetermined life intervals. The various crack patterns would then be combined with a failure criterion to compute the distribution in residual strength for a given point in life. Determining the distributions in residual strength as a function of elapsed cycles would, then, give an indication of how the safe load carrying capability of the structure decays with service usage.

SUMMARY

A probabilistic model that includes the variability in crack size and fatigue crack growth rate has been developed for investigating the fatigue lives of MSD panels. These variables were defined from examples that represent MSD in aging aircraft and represent the properties of the materials that was used to build these aircraft. Six Monte-Carlo simulations were run with variations of fixed and variable conditions for different random variable combinations. The MSD crack size distribution had a dominant effect on the fatigue lives, and the variability in crack growth rate had a lesser effect. The model predicted that the majority of life was spent propagating the MSD cracks until adjacent crack-tips link-up, and then approximately 5% of the panel life remains. The probabilistic model provides an improved understanding of the influences of widespread fatigue cracking on remaining fatigue lives.

ACKNOWLEDGEMENTS

This research was sponsored by the Air Force Office of Scientific Research under grant F49620-93-1-0377.

REFERENCES

1. Yang, J. N.; and Manning, S. D.: Demonstration of Probabilistic-Based Durability Analysis Method for Metallic Airframes. *J. Aircraft*, vol. 27, no. 2, February 1990, pp. 169-175.
2. Manning, S. D.; and Yang, J. N.: USAF Durability Design Handbook: Guidelines for the Analysis and Design of Durable Aircraft Structures. AFWAL-TR-83-3027, Air Force Flight Dynamics Laboratory, WPAFB, OH, January 1984.
3. Manning, S. D.; and Yang, J. N.: Advanced Durability Analysis, Volume I - Analytical Methods. AFWAL-TR-86-3017, Air Force Wright Aeronautical Laboratories, WPAFB, OH, July 1987.
4. Manning, S. D.; and Yang, J. N.: Advanced Durability Analysis, Volume II - Analytical Predictions, Test Results and Analytical Correlations, AFWAL-TR-86-3017, Air Force Wright Aeronautical Laboratories, WPAFB OH, February 1989.
5. Yang, J. N.; and Manning, S. D.: Distribution of Equivalent Initial Flaw Size. 1980 *Proceedings of Annual Reliability and Maintainability Symposium*, January 1980, pp. 112-120.
6. Virkler, D. A.; Hillberry, B. M.; and Goel, P. K.: The Statistical Nature of Fatigue Crack Propagation. AFFDL-TR-78-43, Air Force Flight Dynamics Laboratory, WPAFB, OH, April 1978.
7. Ostergaard, D. F.; and Hillberry, B. M.: Characterization of the Variability in Fatigue Crack Propagation Data. *Probabilistic Fracture Mechanics and Fatigue Methods: Applications for Structural Design and Maintenance*, ASTM STP 798, American Society for Testing and Materials, 1983, pp. 97-115.
8. Moukawsher, E. J.; Neussl, M. A.; and Grandt, A. F., Jr.: A Fatigue Analysis of Panels with Multiple Site Damage. Proceedings of the 1992 USAF Structural Integrity Program Conference, Technical Report WI-TR-4080, Wright Patterson Laboratory, WPAFB, September 1993, pp. 257-273.
9. Moukawsher, E. J.; Neussl, M. A.; and Grandt, A. F., Jr.: Analysis of Panels with Multiple Site Damage. AIAA-94-1459, April 1994.
10. Moukawsher, E. J.: Fatigue Life and Residual Strength of Panels with Multiple Site Damage. M.S. Thesis, School of Aeronautics and Astronautics, Purdue University, West Lafayette, IN, May 1993.
11. Buhler, K.; Grandt, A. F., Jr.; and Moukawsher, E. J.: Fatigue Analysis of Multiple Site Damage at a Row of Holes in a Wide Panel. Advanced Structural Integrity methods for Airframe Durability and Damage Tolerance, NASA CP-3274, 1994.
12. Swift, T.: Damage Tolerance Capability. *Fatigue of Aircraft Materials*, Proceedings of the Specialists Conferences dedicated to the 65th birthday of J. Schijve, 1992, Delft University Editors, Delft University Press, 1992, pp. 351-387.
13. Lincoln, J. W.: Risk Assessment of an Aging Military Aircraft. *J. Aircraft*, vol. 22, no. 8, August 1985, pp. 687-691.

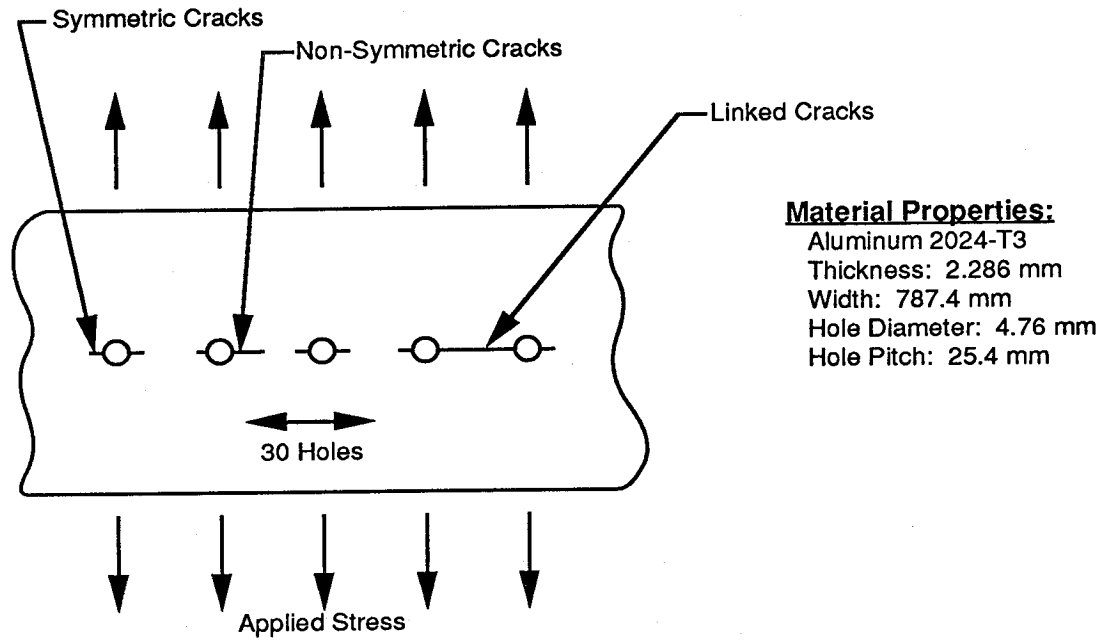


Figure 1: MSD panel.

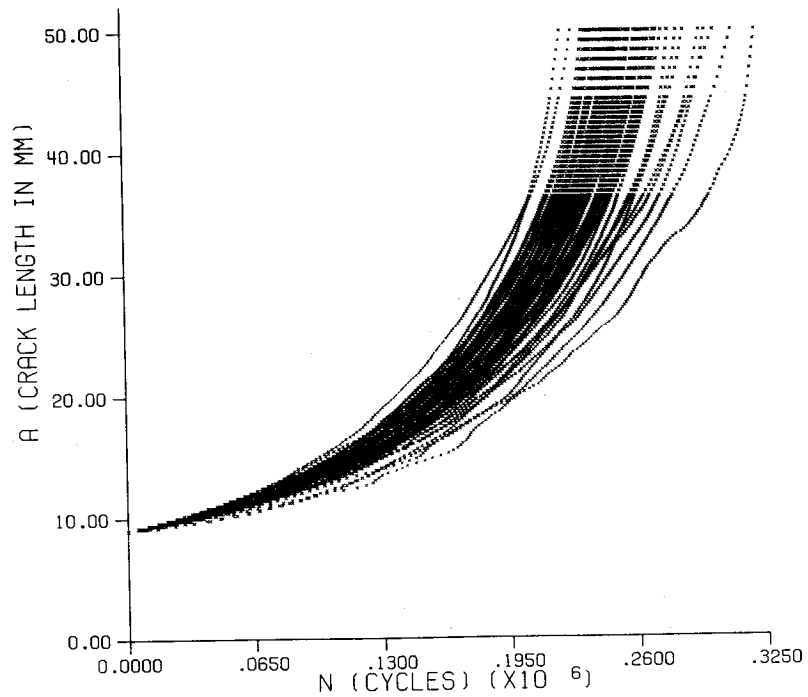


Figure 2: Virkler's data from 68 replicate fatigue crack growth tests in 2024-T3 aluminum alloy specimens.

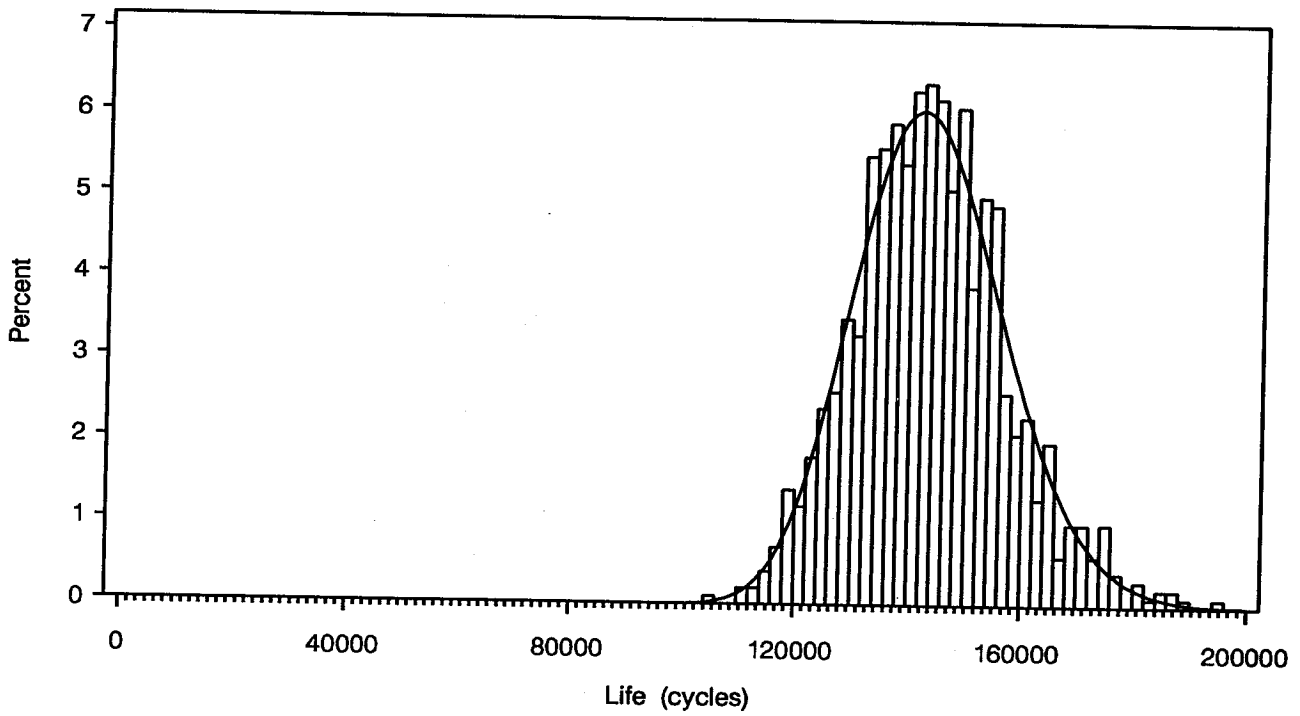


Figure 3: Remaining fatigue life histogram, Case 1: mean size cracks; variable growth parameters for each panel.

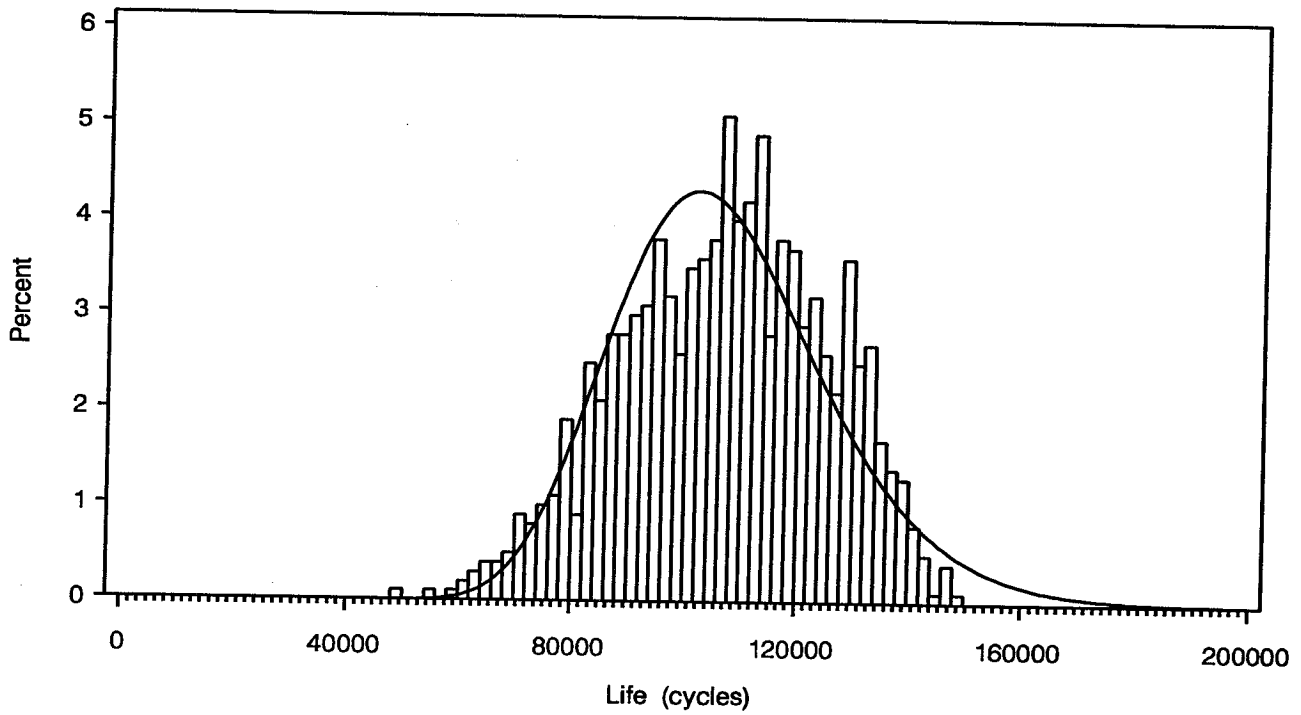


Figure 4: Remaining fatigue life histogram, Case 2: variable symmetric crack-sizes; mean crack growth parameters.

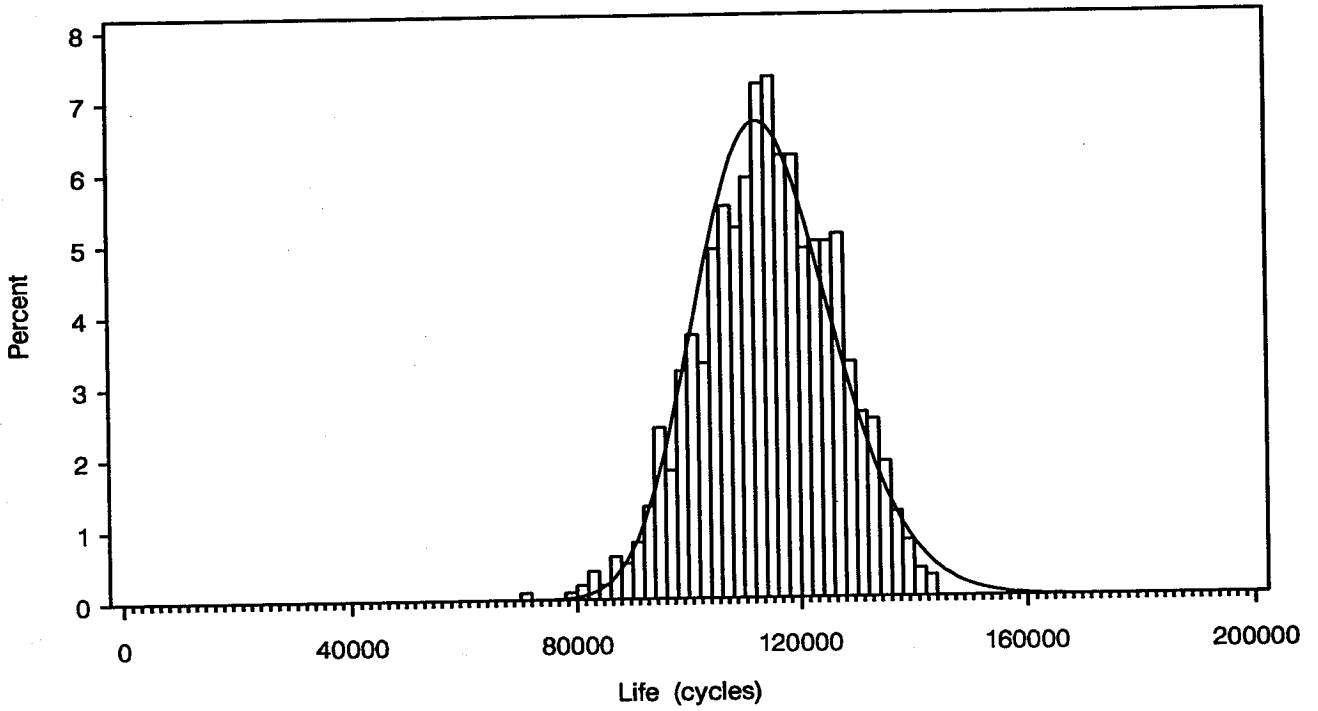


Figure 5: Remaining fatigue life histogram, Case 3: variable unsymmetric crack sizes; mean crack growth parameters for each panel.

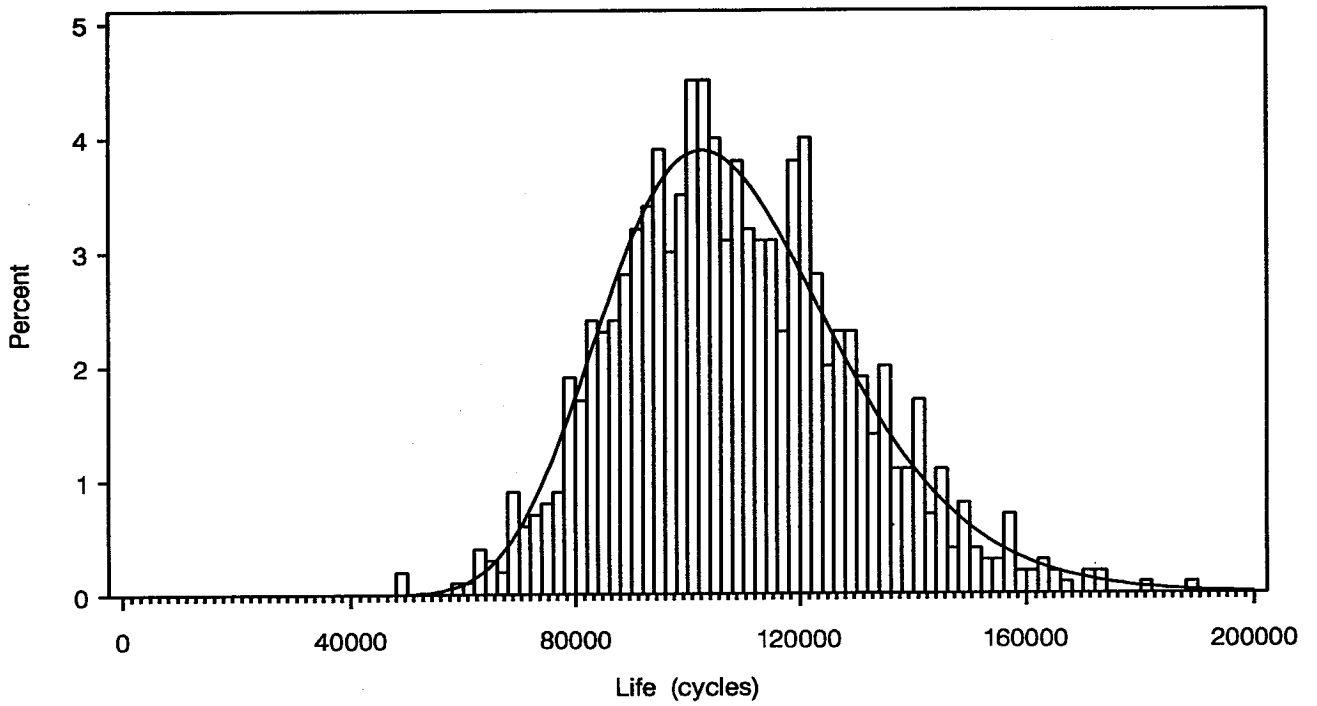


Figure 6: Remaining fatigue life histogram, Case 4: variable symmetric crack sizes; variable crack growth parameters for each panel.

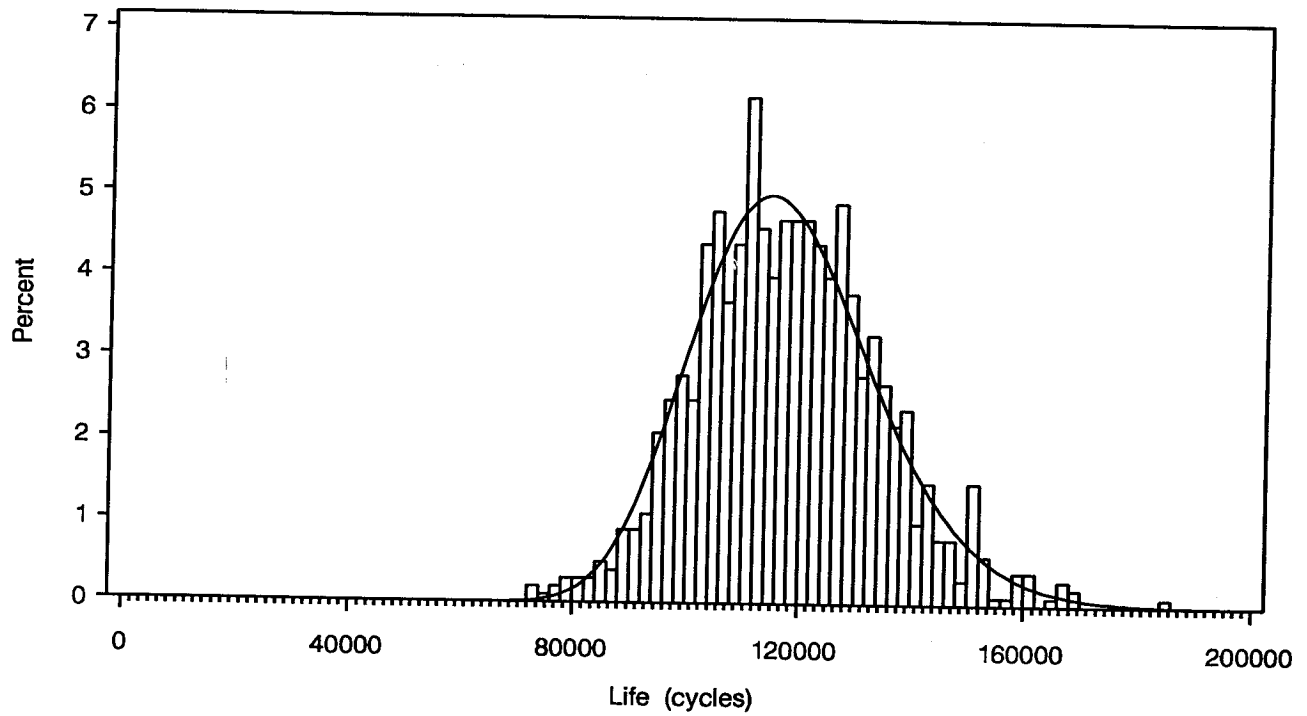


Figure 7: Remaining fatigue life histogram, Case 5: variable unsymmetric crack sizes; variable crack growth parameters for each panel.

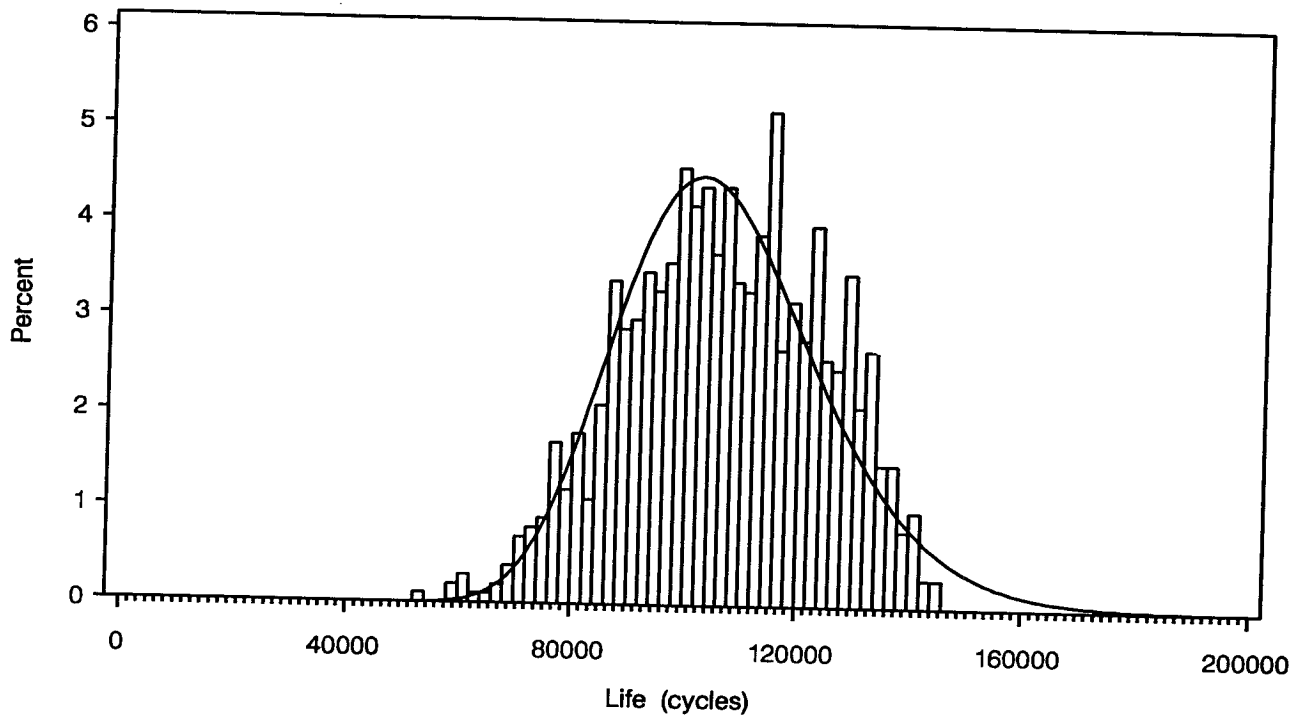


Figure 8: Remaining fatigue life histogram, Case 6: variable symmetric crack sizes; variable crack growth parameters at each hole for each panel (heterogeneous panel).

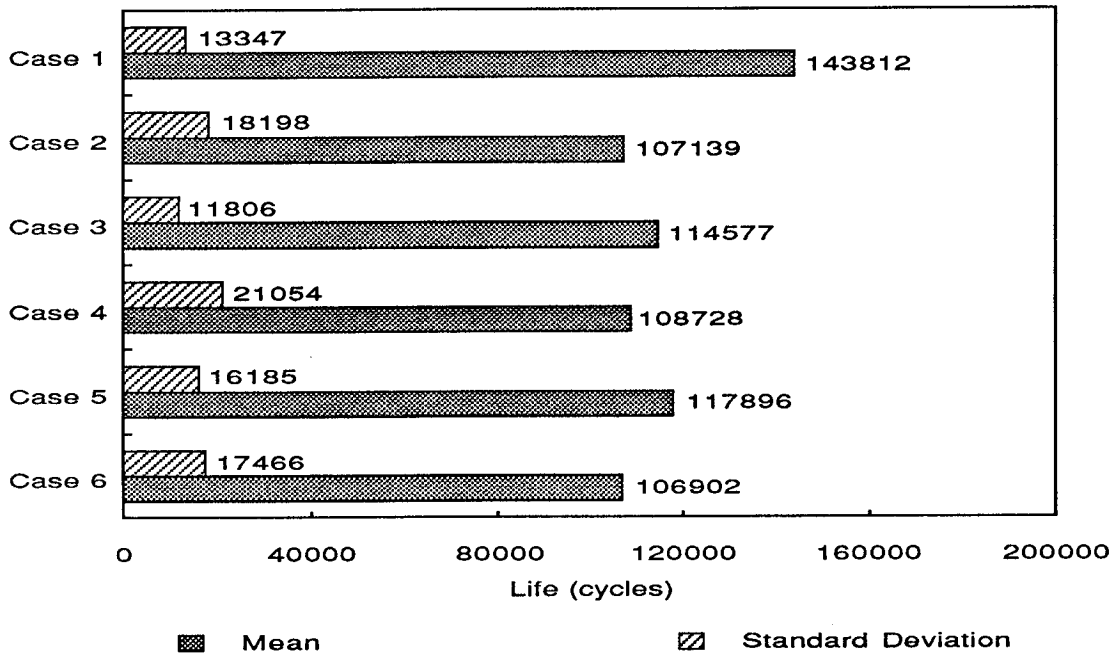


Figure 9: Remaining fatigue life bar chart of mean and standard deviation for Cases 1-6.

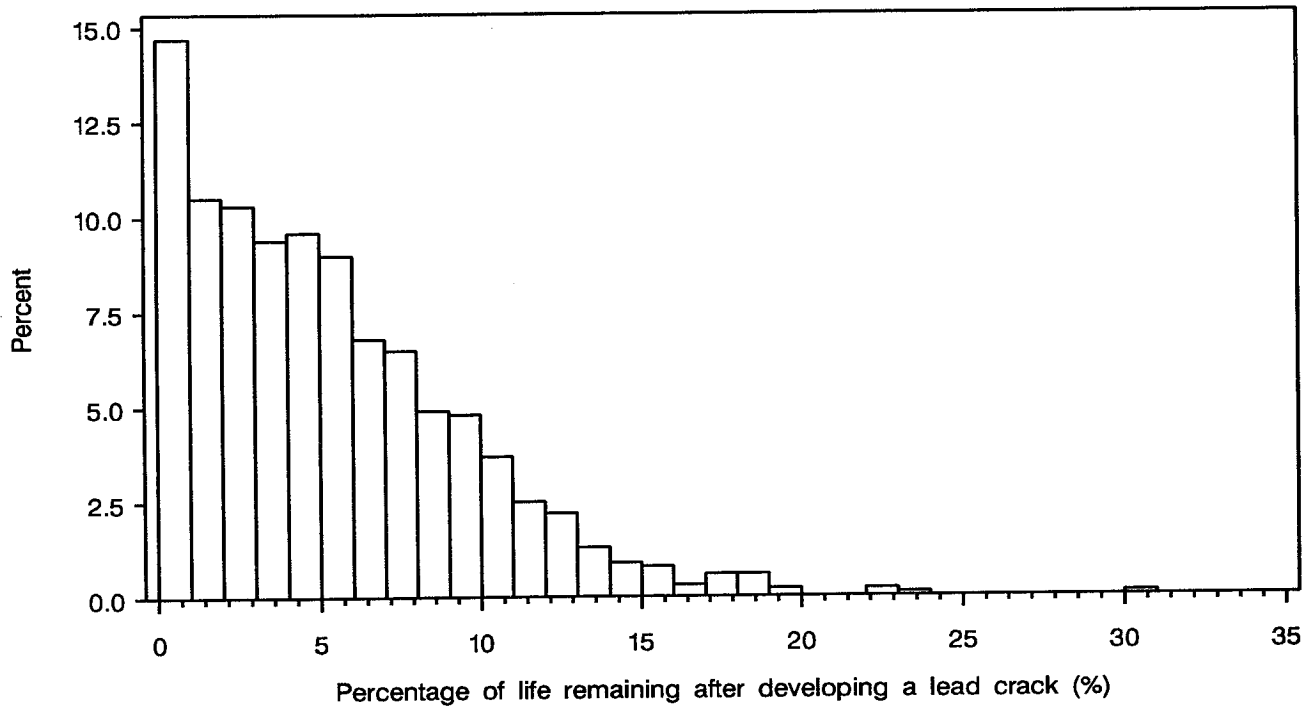


Figure 10: Percent remaining fatigue life histogram after developing a lead crack, Case 2: variable symmetric crack sizes; mean crack growth parameters.

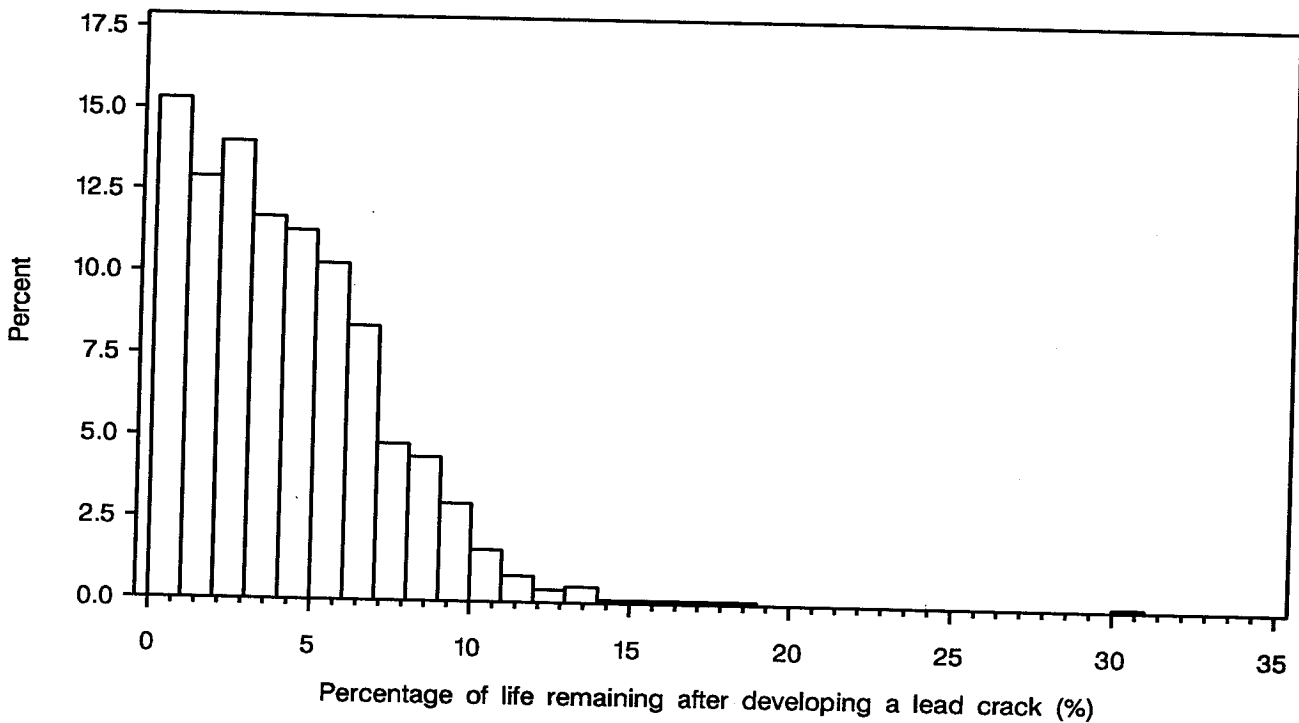


Figure 11: Percent remaining fatigue life histogram after developing a lead crack, Case 3: variable unsymmetric crack sizes; mean crack growth parameters for each panel.

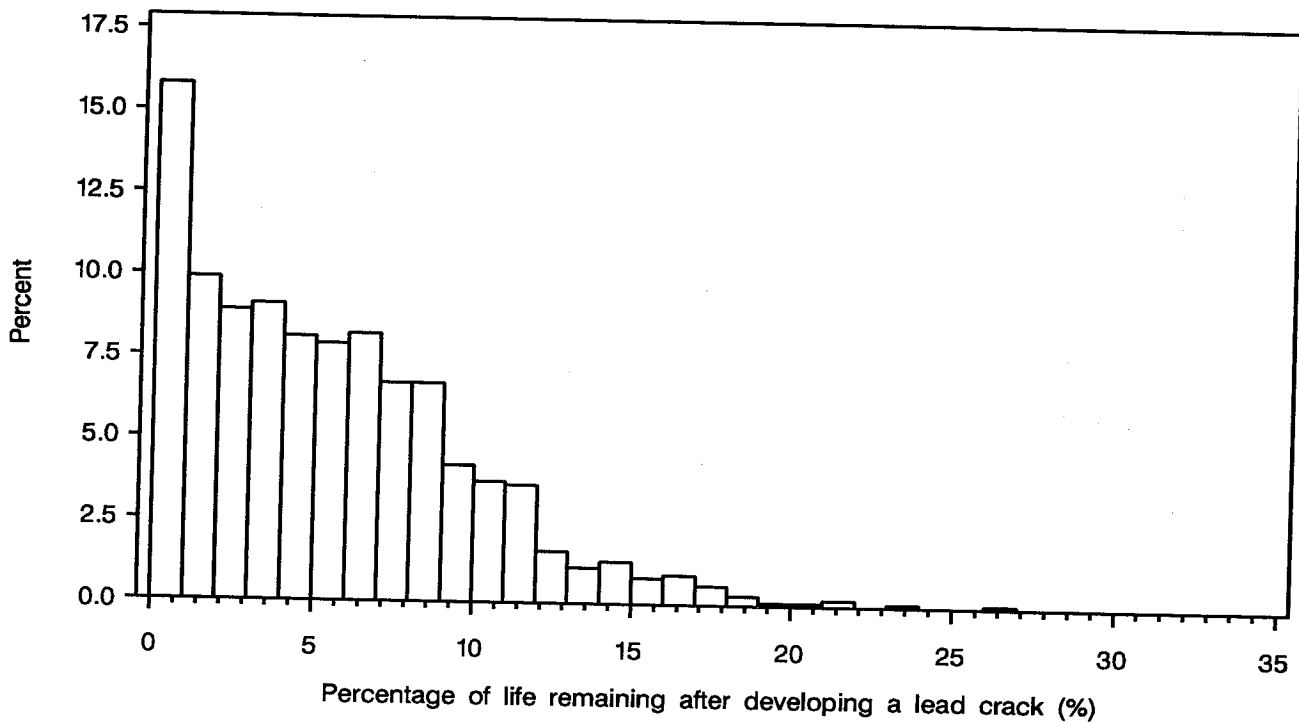


Figure 12: Percent remaining fatigue life histogram after developing a lead crack, Case 4: variable symmetric crack sizes; variable crack growth parameters for each panel.

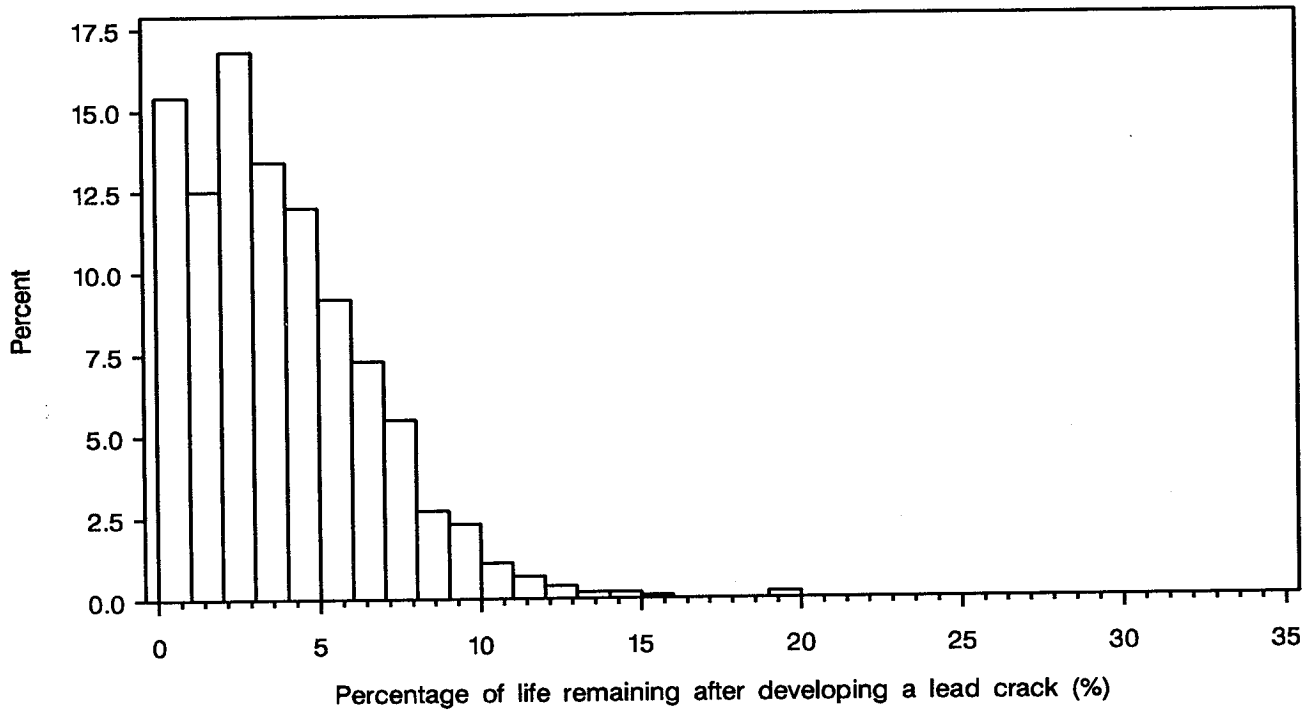


Figure 13: Percent remaining fatigue life histogram after developing a lead crack, Case 5: variable unsymmetric crack sizes; variable crack growth parameters for each panel.

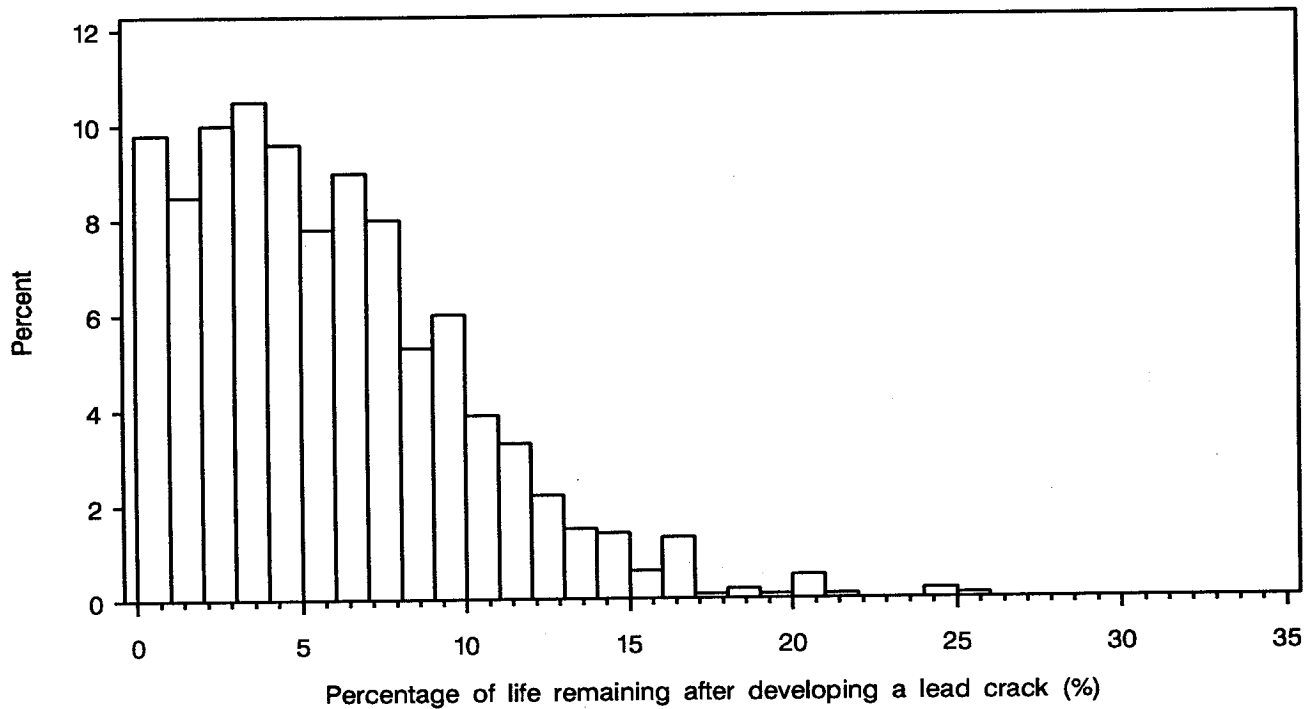


Figure 14: Percent remaining fatigue life histogram, Case 6: variable symmetric crack sizes; variable crack growth parameters at each hole for each panel (heterogeneous panel).

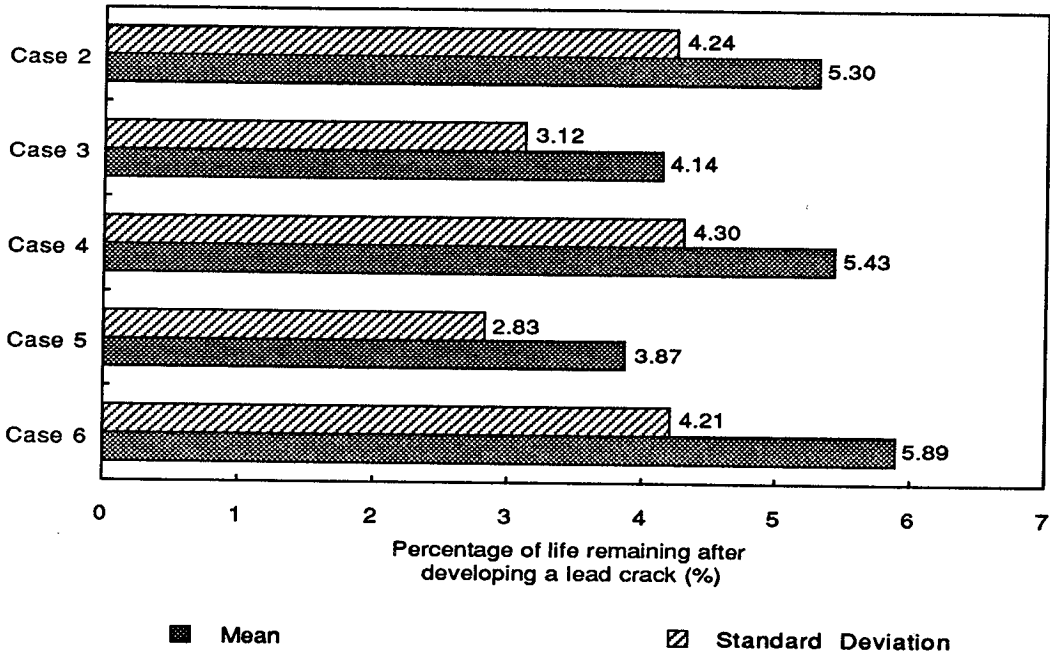


Figure 15: Percent remaining fatigue life bar chart of mean and standard deviation after developing a lead crack (cases 2-6).

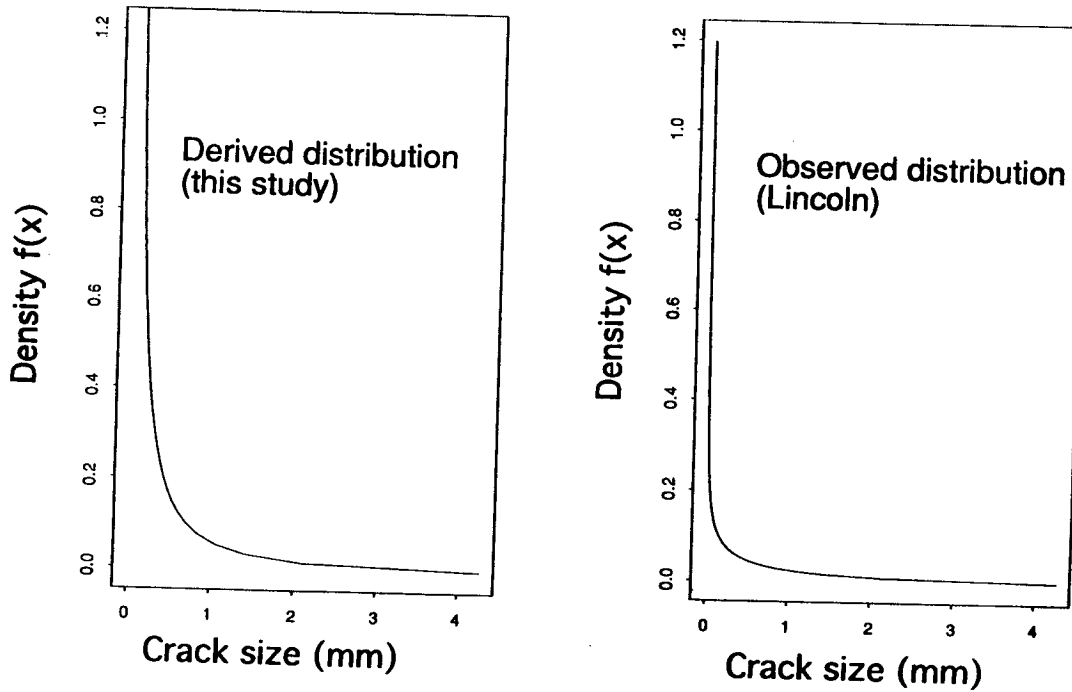


Figure 16: Analytically derived initial crack size distribution compared with observed cracks reported by Lincoln.